# Comparative metabolic flux analysis of an Ashbya gossypii wild type strain and a high riboflavin-producing mutant strain

# Comparative metabolic flux analysis of an *Ashbya gossypii* wild type strain and a high riboflavin-producing mutant strain

Bo-Young Jeong[1], Christoph Wittmann[2], Tatsuya Kato[3], Enoch Y. Park[1,3*]

*Laboratory of Biotechnology, Integrated Bioscience Section, Graduate School of Science and Technology, Shizuoka University, 836 Ohya Suruga-ku Shizuoka 422-8529, Japan,*[1] *Institute of Biochemical Engineering, Braunschweig University of Technology, Gauss Street 17, 38106 Braunschweig, Germany,*[2] *Research Institute of Green Science and Technology, Shizuoka University, 836 Ohya Suruga-ku Shizuoka 422-8529, Japan*[3]

Bo-Young Jeong
E-mail: samsuni11@hotmail.com

Christoph Wittmann
E-mail: c.wittmann@tu-braunschweig.de

Tatsuya Kato
E-mail: atkato@ipc.shizuoka.ac.jp

Enoch Y. Park
E-mail: acypark@ipc.shizuoka.ac.jp

* Corresponding author: Tel. & Fax: +81-54-238-4887. *E-mail address:* acypark@ipc.shizuoka.ac.jp(EYP).

## Abstract

**In the present study, we analyzed the central metabolic pathway of an *A. gossypii* wild type strain and a riboflavin over-producing mutant strain developed in a previous study in order to characterize the riboflavin over-production pathway. $^{13}$C-Metabolic flux analysis ($^{13}$C-MFA) was carried out in both strains, and the resulting data were fit to a steady-state flux isotopomer model using OpenFLUX. Flux to pentose-5-phosphate (P5P) via the pentose phosphate pathway (PPP) was 9% higher in the mutant strain compared to the wild type strain. The flux from purine synthesis to riboflavin in the mutant strain was 1.6%, while that of the wild type strain was only 0.1%, a 16-fold difference. In addition, the flux from the cytoplasmic pyruvate pool to the extracellular metabolites, pyruvate, lactate, and alanine, was 2-fold higher in the mutant strain compared to the wild type strain. This result demonstrates that increased guanosine triphosphate (GTP) flux through the PPP and purine synthesis pathway (PSP) increased riboflavin production in the mutant strain. The present study provides the first insight into metabolic flux through the central carbon pathway in *A. gossypii* and sets the foundation for development of a quantitative and functional model of the *A. gossypii* metabolic network.**



**[Keywords:** *Ashbya gossypii*; Riboflavin; $^{13}$C Metabolic flux analysis; Central carbon metabolism; Mutant]

# INTRODUCTION

Riboflavin (RIB), also known as vitamin $B_2$, is widely distributed in plants and microorganisms, where it serves as a precursor for flavin adenine dinucleotide and flavin mononucleotide synthesis. Flavin adenine dinucleotide and flavin mononucleotide have important cellular roles as co-factors for dehydrogenases and oxidoreductases (1). However, animals, including humans, cannot synthesize RIB, and hence, this nutrient must be supplied through foods and dietary supplements (2, 3). Currently, RIB is produced by fermentation using microorganisms such as the fungi *Ashbya gossypii* and *Eremothecium ashbyii*, the yeast *Candida flaveri*, and the bacterium *Bacillus subtilis* (4). *A. gossypii*, which is capable of RIB overproduction, has been used in industrial RIB production. Importantly, the *Ashbya* genome has already been sequenced and annotated (5), which may accelerate the improvement of RIB production in this organism. In order to improve RIB production, many researchers have developed high RIB-producing *A. gossypii* strains through mutagenesis or metabolic engineering (6–9).

Systems biology combines datasets associated with gene expression, such as those from transcriptomics and proteomics, with data from metabolomics and metabolic flux analysis (MFA, fluxomics) (10). This combination of "omics" techniques potentially represents the most powerful approach for understanding and manipulating cellular metabolism (10, 11). $^{13}$C-MFA provides a direct measure of the metabolic phenotype by quantitatively analyzing *in vivo* carbon flux in metabolic networks (12). Cells are incubated with a carbon isotope ($^{13}$C)-labeled precursor, and the $^{13}$C-labeling data in metabolic intermediates and end-products are measured and thier deviation between simulation and experiment is minimized by iterative variation of the free fluxes until the optimum fit is obtained (13, 14). Fluxes from $^{13}$C mass isotopomer data and extracellular flux measurements are fit to a steady-state flux isotopomer model using OpenFLUX based on the Elementary Metabolite Units (EMU) decomposition

algorithm (15, 16). OpenFLUX has previously been used for $^{13}$C-MFA of lysine-producing *Corynebacterium glutamicum* and succinate-producing *Basfia succiniciproducens* (17, 18). However, it has never been used for fungal metabolic flux analysis.

The metabolism of RIB over-production in *A. gossypii* is a matter of great interest because this fungus has been used for industrial RIB production. However, despite numerous studies, a clear and unequivocal description of fluxomics in *A. gossypii* has not yet been provided. Here, $^{13}$C-MFA was performed in an *A. gossypii* wild type strain and a RIB over-producing mutant strain, and differences in metabolism between the wild type and mutant strains were analyzed. The present study revealed differences in carbon metabolic flux in the RIB-producing phase between the wild type and mutant strains.

## MATERIALS AND METHODS

**Strains and maintenance** The *A. gossypii* wild type strain ATCC 10895 and the *A. gossypii* mutant strain W122032 were used in this study. The *A. gossypii* mutant strain was isolated by disparity mutagenesis in our previous study and was shown to produce RIB at levels nine-fold higher than the wild type strain when vegetable oil was used as the sole carbon source (6). Both strains were maintained as frozen spore suspensions in 10% (w/v) glycerol at -80°C. Batch cultures were maintained in 500-mL baffled shake flasks containing 50 mL of growth medium on a rotary shaker at 28°C with agitation at 120 rpm.

**Media** YD medium (pH 6.8) containing 10 g/L yeast extract and 10 g/L glucose was used for glycerol stocks. The seed culture and preculture were maintained in complex medium containing 20 g/L glucose, 25 g/L corn steep liquor (CSL), 1.0 g/L $K_2HPO_4$, and 5.0 g/L peptone (19). The main cultivation was performed in chemically defined minimal medium (pH 6.8) containing 50 mM glucose as a carbon source, 1.5 g/L asparagine, 0.75 g/L

$KH_2PO_4$, 0.1 g/L myo-inositol, and mineral ions (4.4 mg/L $CoCl_2 \cdot 6H_2O$, 18.0 mg/L $MnCl_2 \cdot 4H_2O$, 44.0 mg/L $ZnSO_4 \cdot 7H_2O$, 10.1 mg/L $MgSO_4 \cdot 7H_2O$, 27.0 mg/L $FeCl_3 \cdot 6H_2O$, 21.9 mg/L $CaCl_2 \cdot 6H_2O$, and 2.7 mg/L $CuSO_4 \cdot 5H_2O$). The stock solution for the mineral ions was autoclaved separately for 20 min at 121°C and cooled to room temperature prior to addition. All chemicals were of analytical grade and were purchased from Fluka (Buchs, Switzerland), Merck (Darmstadt, Germany), or Sigma (St. Louis, USA). For tracer experiments, naturally labeled glucose was replaced with 99% [1, 2-$^{13}$C] glucose (99%, Cambridge Isotope Laboratories, Andover, USA). To resolve the metabolic fluxes of interest, two parallel experimental set-ups were chosen for the labeling studies (20).

**Cultivation** Seed culture and preculture were incubated in complex medium (21) for 48 and 72 h, respectively, at 28°C. *A. gossypii* strains from glycerol stocks (10% *v/v*) were used for seed culture and were used to inoculate 10 mL complex medium in 100-mL baffled shake flasks. The seed culture was then used to inoculate the preculture (10% *v/v*). Subsequently, the cells were harvested by centrifugation at 1006 × *g* for 10 min, washed with sterile distilled water, and used to inoculate the main culture in a 500-mL baffled shake flask containing 50 mL minimal medium. Physiological studies of the quantification of growth and production characteristics were performed using triplicate cultures. Cultures incubated with tracer $^{13}$C-labeled GLC were maintained in 100-mL baffled shake flasks containing 10 mL minimal medium. All cultures were inoculated with exponentially growing cells from the preculture and were incubated at 28°C and agitated at 120 rpm on a rotary shaker (Certomat BS-1/50 mm, Sartorius, Göttingen, Germany).

**Measurements of dry cell weight (DCW) and extracellular metabolites** DCW was measured in triplicate. Harvested cells were washed twice with sterile distilled water and then

dried at 100°C until a constant weight was reached. For quantification of organic acids and glucose the culture supernatants were filtered microfilter (Minisart 0.2 µm, Sartorius). Organic acid was measured by HPLC (Elite Lachrome HITACHI Ltd., Japan) using a Metacarb 67H column (250 mm × 4.6 mm, 5 µm, VWR-Hitachi, Darmstadt, Germany) with 1 mM $H_2SO_4$ as the mobile phase and a flow rate of 0.8 mL/min at 70°C. Glucose was measured using a biochemical analyzer (YSI 2700 SELECT, Ohio, USA). To quantify RIB concentration, 0.8 mL of the culture broth was thoroughly mixed with 0.2 mL 1 N NaOH. A 0.4-mL aliquot of the resulting solution was neutralized with 1 mL 0.1 M potassium phosphate buffer (pH 6.0), and the optical density of the solution at a wavelength of 444 nm was measured. The RIB concentration was calculated using a conversion factor of 127.297 mg-RIB·(L · unit of optical density)$^{-1}$ (22).

**$^{13}$C-Labeling analysis** MFA with GC-MS is usually performed as stationary flux analysis, whereby the metabolism is in metabolic and isotopomer steady state. For $^{13}$C-MFA, cells from the tracer culture were harvested at 7 d of culture time by filtration of 5 mL of culture using a cellulose acetate filter (pore size, 20 µm; Sartorius). After removal of excess medium by washing twice with cold distilled water, the pellets were resuspended in 500 µl 6 M HCl and incubated for 24 h at 100°C to hydrolyze proteins. The hydrolysates were clarified by filtration (0.2 µm, Ultrafree MC, Millipore, Bedford, MA, USA) and dried under nitrogen gas. The resulting proteinogenic amino acids were resolved by the addition of 50 µl dimethylformanide (Sigma, USA) and 0.1% pyridine (Sigma, USA) and were derivatized using 50 µl of the silylation reagent, *N*-methyl-*N*-(*tert*-butyl-dimethylsilyl)-trifluoroacetamide (MBDSTFA) (Macherey-Nagel, Düren, Germany), at 80°C for 30 min prior to gas chromatography and mass spectrometry (GC-MS) analysis. Analysis of the labeling pattern of amino acids from the hydrolyzed cellular protein was carried out using GC-MS (HP Agilent 7890 Gas Chromatograph, Quadrupole Mass Selective Detector 5973;

Agilent Technologies, Waldbronn, Germany). All of the samples were measured first in scan mode, thereby excluding isobaric interference. For enhanced data analysis, the relative fractions of the mass isotopomers of interest were then analyzed in duplicate in selective ion monitoring (SIM) mode (16).

**Metabolic flux modeling and metabolic flux calculations** The metabolic network model of the central metabolism of RIB-producing *A. gossypii* cells was reconstructed based on a previously described model (23, 24), which is based on the compartmentalized metabolic network of *Saccharomyces cerevisiae* based on previous reports. The model consists of *A. gossypii* central carbon metabolic pathways, including glycolysis, the PPP, the TCA cycle, and the PSP, which was constrained using the measured extracellular uptake fluxes, as well as intracellular fluxes estimated from the $^{13}C$ isotopomer data. The cytosol and the mitochondrion were regarded as separate compartments, and separate pools for pyruvate, oxaloacetate, and acetyl CoA were included in each of the two compartments. The pathways of anabolism, including amino acid, organic acid, and RIB biosynthesis, were revised by inspection of metabolic flux studies in different bacteria (25, 26), yeasts, and other fungi (27–29). Metabolic flux was calculated using the yield coefficients based on the metabolic network reactions. Fifty-eight stoichiometric reactions, including uptake reactions for GLC ($V_1$) and ASN ($V_2$), were considered. Taking biomass concentration and measured physiological yield coefficients into account, 13 measurements of flux from anabolic precursors into biomass were included (Supplementary Table S1). Overall, 24 metabolite balances were formulated from stoichiometric reactions (Supplementary Table S2). A total of 83 reactions were considered in order to construct a metabolic network model of $^{13}C$-MFA of *A. gossypii* (Supplementary Table S3). All flux values were normalized with respect to the glucose uptake rate. Metabolic flux values were estimated using the MATLAB-based modeling software OpenFLUX (15). Statistical analysis of the resulting fluxes was carried

Supp. Tables S1, S2 and S3

out using a Monte Carlo approach (20), which is capable of providing precise information regarding the error distributions of flux parameters.

## RESULTS

**Growth and RIB production by *A. gossypii* wild type and mutant strains** The time course for cell growth and consumption of glucose (GLC) and asparagine (ASN) by wild type and mutant *A. gossypii* cultures is shown in Fig. 1A and B. Growth was coupled with consumption of GLC and ASN. The amount of ASN consumed by the wild type strain was 5 times higher than that of the mutant strain, but RIB production was 10-fold less in the wild type strain compared to the mutant (Fig. 1A). RIB production by *A. gossypii* has been reported to start at the end of the growth phase linked to sporulation in wild type cells (30). In contrast, RIB production of the mutant strain was found to begin at the beginning of exponential growth. In addition, the concentration of lactate (LAC) in the mutant strain was significantly increased compared to the wild type strain (Fig. 1B). Fig. 1

Production of RIB as a product and LAC as a by-product was measured and correlated with the amount of GLC consumed. The yields of RIB and LAC were calculated during the exponential growth phase for each strain when cultured on chemically defined minimal medium. The biomass yields based on consumed GLC were 0.047 and 0.063 g DCW/mmol GLC for the *A. gossypii* wild type and mutant strains, respectively. The specific rates of cell growth, GLC and ASN consumption, and RIB and LAC production of the wild type and mutant strains during the exponential growth phase were shown in Table 1. The RIB, LAC, acetate (ACE), alanine (ALA), and pyruvate (PYR) yields based on GLC consumed were higher in the mutant than in the wild type strain. The RIB yield, $Y_{RIB/GLC}$ was 16-fold higher in the mutant compared to the wild type. It is also notable that $Y_{LAC/GLC}$ and $Y_{PYR/GLC}$ were 4.4 and 2.9 times higher in the mutant strain than in the wild type strain. In contrast, the alpha- Table 1

ketoglutarate (AKG), glutamate (GLU), and succinate (SUC) yields in the mutant strain were relatively lower compared to the wild type strain. The overall yield coefficients for the mutant were significantly different from the wild type under the same culture conditions. The primary differences observed were in production of RIB and its main by-products, including LAC and PYR from the pyruvate pool.

**Construction of the metabolic network of *A. gossypii*** To quantify metabolic flux, [1, 2-$^{13}$C]-labeled GLC and unlabeled ASN were used as the sole carbon and nitrogen sources, respectively. Physiological yield coefficients (Table 1) and measured mass isotopomer fractions (Tables 2 and 3) were calculated for construction of related metabolic flux models.

RIB is produced by *A. gossypii* cells cultured on medium containing vegetable oil as a sole carbon source through the β-oxidation pathway, the glyoxylate cycle, the TCA cycle, gluconeogenesis, the pentose phosphate pathway (PPP), the purine synthesis pathway (PSP), and the RIB synthesis pathway (1, 31). In contrast, when GLC is used as a carbon source, RIB is produced through glycolysis (the Embden-Meyerhof-Parnas pathway, EMP), the PPP, the PSP, and the RIB synthesis pathway. In this study, the metabolic model for growth of *A. gossypii* on GLC minimal medium was constructed. In this model, the β-oxidation pathway, glyoxylate cycle, and other pathways were omitted due to the use of GLC as a carbon source.

**Analysis of metabolic fluxes of *A. gossypii* wild type and mutant strains** The corresponding stoichiometric matrix was calculated, and the results revealed that all metabolic balances were linearly independent. Together with the 43 mass isotopomer fractions (Tables 2 and 3), stoichiometric reactions and carbon fluxes into biomass were available for analysis of metabolic flux. The intracellular flux distributions of wild type and mutant strains are shown in Fig. 2. The relative metabolic fluxes were normalized with respect to the specific GLC uptake rate. Glycolysis and the PPP were used for catabolic and anabolic metabolism of GLC, respectively. In wild type *A. gossypii*, 30% of G6P was

converted to P5P via the PPP, whereas 65.7% was channeled through the EMP. In contrast, 39.2% of G6P was used to generate P5P via the PPP, and 57.1% was channeled through the EMP in the *A. gossypii* mutant strain. The excess carbon in the PPP, totaling 9.2% in *A. gossypii* wild type strain and 11.7% in the mutant strain, was channeled back to the EMP via F6P and GAP. Carbon flux to the PPP in the mutant strain was not significantly increased compared to that of the wild type strain. In contrast, the flux from the cytosolic pyruvate ($PYR_{cyt}$) pool to extracellular pools of PYR, LAC, and ALA ($PYR_{ex}$, $LAC_{ex}$, and $ALA_{ex}$) in the mutant strain was 31.6%, a two-fold increase over the wild type strain. The flows of $PYR_{cyt}$ to the extracellular $PYR_{ex}$, $LAC_{ex}$, and $ALA_{ex}$ pools in the mutant strain were 16.8%, 6.6%, and 1.8%, respectively, representing a 2–4 fold increase compared to the wild type strain. Consistent with these observations, the intracellular flows of $PYR_{cyt}$ to $OAA_{cyt}$ in the mutant strain were 30.4%, while those in the wild type were 49.1%. Thus, the overall fluxes associated with the EMP in the wild type strain were more connected with the TCA cycle than those in the mutant strain.

The $ASN_{ex}$ flux in the *A. gossypii* wild type strain was 39.4%, which was higher than that of the mutant. The major fraction of ASN was channeled through aspartate (ASP) into the TCA cycle, and the resulting $OAA_{cyt}$ formed through anaplerosis was transported into the mitochondria oxaloacetate ($OAA_{mit}$). The carbon flux from $OAA_{cyt}$ into the TCA cycle in the wild type strain was 84.5%, but it was 57.5% in the mutant strain. In addition, the normal flux from SER and THR to GLY was 1.3% in the wild type strain, while it was 3.4% in the mutant, suggesting that the mutant strain was more active in supplying GLY. Usually, RIB production by *A. gossypii* is limited by GLY, an early precursor that is required in the PSP (31). GTP is derived from the precursors GLY and P5P (32). Consequentially, this flux analysis indicated that the supply of GTP in the mutant strain was higher than that in the wild type strain, which led to improved RIB production in the mutant in parallel with increased

LAC production.

## DISCUSSION

*A. gossypii* cultured in complex medium can utilize vegetable oils as a carbon source for RIB production, and these oils can be metabolized through the glyoxylate cycle and β-oxidation (33). However, in this study, the relative flux of carbon through all metabolic pathways except the glyoxylate cycle and β-oxidation was investigated because GLC was used as a carbon source. The mutant, RIB-overproducing strain grew more slowly ($\mu = 0.78$ $d^{-1}$) than the control strain ($\mu = 1.01$ $d^{-1}$) and required a 1-day lag phase. To compare carbon flux between the *A. gossypii* wild type and mutant strains, based on the flux distributions, approximately 39.2% of carbon from GLC was channeled into the PPP in the *A. gossypii* mutant, which was higher than that of the wild type (30%). In TCA cycle, pyruvate flux in the mutant strain was 20% lower than that in the wild type. Carbon flux from purine synthesis to RIB in the mutant strain was 16-fold higher than that in the wild type strain, which agreed with the 16-fold higher RIB yield of the mutant that that of wild type. This result demonstrates that increased GTP flux through the PPP and PSP increased RIB production in the mutant strain. This study confirmed that GLY and folate derivative production is critical for RIB production in *A. gossypii*, as the flux in the mutant was directed to production of GLY and a folate derivative, 5, 10-methylenetetrahydrofolate in parallel with its RIB production (34). GLY is the precursor for GTP, which is a precursor for folate, and another folate derivative, 10-formyltetrahydrofolate, is utilized in purine metabolism as a C1 carbon carrier. ASN, which was used as the sole nitrogen source in this study, is also utilized in purine metabolism for the production of phosphoribosylaminoimidazole-succinocarboxamide. In addition, ASN might be used as carbon source. Therefore, $OAA_{cyt}$ and THR made from ASN were constructed into the metabolic model. These results suggest that the PSP is

connected to GLY, folate, and ASN metabolism for RIB production in *A. gossypii*. The phosphoribosylaminoimidazole-succinocarboxamide synthase (ADE1, AER221Wp) expression in the mutant has been shown to be enhanced more than 5-fold over wild type strain during RIB production in a complex medium containing yeast extract and rapeseed oil (6). Thus, the results of this study are in agreement with previous proteomics results for the mutant strain used in this study. Interestingly, in the mutant strain, $LAC_{ex}$ was highly over-produced as a result of increased flux from the $PYR_{cyt}$ pool.

$^{13}$C-MFA based on OpenFLUX was carried out to compare the central metabolism in high RIB-producing *A. gossypii* between wild type strains. However, we found large differences between estimated and measured relative mass isotopomer distributions of metabolites in both strains (Tables 2 and 3). The residual sum of squares (RSS) in wild type and mutant were 0.034 and 0.047, respectively, suggesting that the used model in this study is not reliable enough to analyze RIB producing MFA in *A. gossypii* in detail. Therefore, we set V8-13, V19, V29, V32 and V33 as reversible reactions to refine this metabolic network. The relative mass isotopomer distributions of metabolites in both strains were recalculated, and resulting RSS values in wild type and mutant were 0.044 and 0.030, respectively. This indicates that other factors affected the accuracy of the flux distribution. More detailed analysis of MFA in *A. gossypii* strain requires more accurate MFA method with various respects.

In the present study, *A. gossypii* metabolic flux analysis was investigated using $^{13}$C-MFA in order to compare metabolic flux between the wild type and mutant strains. Carbon flux from purine synthesis to RIB in the mutant strain was 16-fold higher than that in the wild type strain. This result demonstrates that increased GTP flux through the PPP and PSP increased RIB production in the mutant strain. In order to improve RIB production it is one option to reinforce gene expressions related to PPP and PSP pathways. On the other hand,

industrial RIB producer uses vegetable oil as carbon source, meaning glyoxylate cycye is important. Unfortunately in this work we can't reveal carbon flux of glyoxylate cycle, but if it is available it would be possible to increase oil consumption for RIB improvement. Because it is easy to identify mutated genes of RIB-overproducing mutant by genome analysis. Although $^{13}$C-MFA based on OpenFLUX was not highly accurate in *A. gossypii*, analysis of carbon flux from the EMP to the RIB synthesis pathway revealed important differences between the *A. gossypii* wild type and mutant strains. These results set the stage for further rational development of new RIB-overproducing strains.

## References


1. **Kato, T. and Park, E.Y.:** Riboflavin production by *Ashbya gossypii*, Biotechnol. Lett., **34,** 611–618 (2011).
2. **Cooperman, J.M. and Lopez, R.:** Riboflavin. In: Handbook of vitamins. Edited by Machlin, L.J., Dekker, New York, 300–327 (1984).
3. **Eggersdorfer, M., Adam, G., John, M., Hähnlein, W., Labler, L., Baldenius, R.U., Bussche-Hünnefeld, L., Hilgemann, E., Hoppe, P., Stürmer, R., and other 19 authors:** Vitamins. In: Ullmann's encyclopedia of industrial chemistry, VCH, Weinheim, A27, 443–613 (1996).
4. **Stahmann, K.P., Revuelta, J.L., and Seulberger, H.:** Three biotechnical processes using *Ashbya gossypii, Candida famata,* or *Bacillus subtilis* compete with chemical riboflavin production. Appl. Microbiol. Biotechnol., **53,** 509–516 (2000).
5. **Dietrich, F.S., Voegeli, S., Brachat, S., Lerch, A., Gates, K., Steiner, S., Mohr, C., Pohlmann, R., Luedi, P., and Choi, S.:** The *Ashbya gossypii* genome as a tool for mapping the ancient *Saccharomyces cerevisiae* genome, Science, **304**, 304–307 (2004).
6. **Park, E.Y., Ito. Y., Nariyama. M., Sugimoto. T., Lies. D., and Kato. T.:** The improvement of riboflavin production in *Ashbya gossypii* via disparity mutagenesis and

DNA microarray analysis, Appl. Microbiol. Biotechnol., **91,** 1315–1326 (2011).

7. **Jiménez, A., Santos, M.A., Pompejus, M., and Revuelta, J.L.:** Metabolic engineering of the purine pathway for riboflavin production in *Ashbya gossypii,* Appl. Environ. Microbiol., **71,** 5743–5751 (2005).
8. **Park, E.Y., Zhang, J.H., Tajima, S., and Dwiarti, L.:** Isolation of *Ashbya gossypii* mutant for an improved riboflavin production targeting for biorefinery technology, J. Appl. Microbiol., **103,** 468–476 (2007).
9. **Tajima, S., Itoh, Y., Sugimoto, T., Kato, T., and Park, E.Y.:** Increased riboflavin production from activated bleaching earth by a mutant strain of *Ashbya gossypii*, J. Biosci. Bioeng., **108,** 325–329 (2009).
10. **Krömer, J., Quek, L.E., and Nielsen, L.:** $^{13}$C-Fluxomics: A tool for measuring metabolic phenotypes, Austrialian Biochemist, **40,** 17–20 (2009).
11. **Lee, S.Y., Lee, D.Y., and Kim, T.Y.:** Systems biotechnology for strain improvement, Trends Biotechnol., **23,** 349–358 (2005).
12. **Niklas, J., Schneider, K., and Heinzle, E.:** Metabolic flux analysis in eukaryotes, Curr. Opin. Biotechnol., **21,** 63-69 (2010).
13. **Kruger, N.J., Masakapalli, S.K., and Ratcliffe, R.G.:** Strategies for investigating the plant metabolic network with steady-state metabolic flux analysis: lessons from an Arabidopsis cell culture and other systems, J. Exp. Bot., **63,** 2309-2323 (2012).
14. **Wittmann, C.:** Fluxome analysis using GC-MS, Microb. Cell Fact., **6**:6 (2007).
15. **Quek, L.E., Wittmann, C., Nielsen, L.K., and Krömer, J.O.:** OpenFLUX: Efficient modeling software for $^{13}$C-based metabolic flux analysis. Microb. Cell Fact., **8**:25 (2009).
16. **Antoniewiz, M.R., Kelleher. J.K., and Stephanopoulos, G.:** Elementary metabolite units (EMU): a novel framework for modeling isotopic distributions, Metab. Eng., **9,** 68-

86 (2007).

17. **Srour, O., Young. J.D., and Eldar, Y.C.:** Fluxomers: a new approach for $^{13}C$ metabolic flux analysis, BMC Sys. Biol., **5**:129 (2011).

18. **Becker, J., Reinefeld, J., Stellmacher, R., Schäfer, R., Lange, A., Meyer, H., Lalk,, M., Zelder, O., von Abendroth, G., Schröder, H., Haefner, S., and Wittmann, C.:** System-wide analysis and engineering of metabolic pathway fluxes in bio-succinate producing *Basfia succiniciproducens*, Biotechnol. Bioeng., **110,** 3013-3023 (2013).

19. **Mateos, L., Jiménez, A., Revuelta, J.L., and Santos, M.A.:** Purine biosynthesis, riboflavin production, and trophic-phase span are controlled by a Myb-related transcription factor in the fungus *Ashbya gossypii*, Appl. Environ. Microbiol., **72,** 5052–5060 (2006).

20. **Wittmann, C. and Heinzle, E.:** Genealogy profiling through strain improvement by using metabolic network analysis: Metabolic flux genealogy of several generations of lysine producing *Corynebacteria*, Appl. Environ. Microbiol., **68,** 5843–5859 (2002).

21. **Goodman, J.J. and Ferrera, R.R.:** Synthesis of riboflavin by *Ashbya gossypii* grown in a synthetic medium, Mycologia, **46**, 556–563 (1954).

22. **Sauer, U., Hatzimanikatis, V., Hohmann, H.P., Manneberg, M., van Loon, A.P., and Bailey, J.E.:** Physiology and metabolic fluxes of wild type and riboflavin-producing *Bacillus subtilis*, Appl. Environ. Microbiol., **62,** 3687–3696 (1996).

23. **Gombert, A.K. and Nielsen, J.:** Mathematical modeling of metabolism, Curr. Opin. Biotechnol., **11,** 180–186 (2000).

24. **Gombert, A.K., dos Santos, M.M., Christensen, B., and Nielsen, J.:** Network identification and flux quantification in the central metabolism of *Saccharomyces cerevisiae* under different conditions of glucose repression, J. Bacteriol., **184,** 1441–1451 (2001).

25. **Dauner, M. and Sauer, U.:** Stoichiometric growth model for riboflavin-producing *Bacillus subtilis*, Biotechnol. Bioeng., **76,** 132–143 (2001).
26. **Kayser, A., Weber, J., Hecht, V., and Rinas, U.:** Metabolic flux analysis of *Escherichia coli* in glucose-limited continuous culture. I. Growth-rate-dependent metabolic efficiency at steady state, Microbiology, **151,** 693–706 (2005).
27. **Frick, O. and Wittmann, C.:** Characterization of the metabolic shift between oxidative and fermentative growth in *Saccharomyces cerevisiae* by comparative $^{13}C$ flux analysis, Microb. Cell Fact., **4**:30 (2005).
28. **Nagamori, E., Shimizu, K., Fujita, H., Tokuhiro, K., Ishida, N., and Takahashi, H.:** Network formation through active migration of human vascular endothelial cells in a multilayered skeletal myoblast sheet, Bioprocess Biosyst. Eng., **36,** 1261–1265 (2012).
29. **Papini, M., Nookaew, I., Siewers, V. and Nielsen, J.:** Physiological characterization of recombinant *Saccharomyces cerevisiae* expressing the *Aspergillus nidulans* phosphoketolase pathway: validation of activity through $^{13}C$-based metabolic flux analysis, Appl. Microbiol. Biotechnol., **95,** 1001–1010 (2012).
30. **Stahmann, K.P., Arst, H.N., Althöfer, H., Revuelta, J.L., Monschau, N., Schlüpen, C., Gätgens, C., Wiesenburg, A., and Schlösser, T.:** Riboflavin, overproduced during sporulation of *Ashbya gossypii*, protects its hyaline spores against ultraviolet light, Environ. Microbiol., **3,** 545–550 (2001).**Ledesma-Amaro, R., Kerkhoven, E.J., Revuelta, J.L., and Nielsen, J.:** Genome scale metabolic modeling of the riboflavin overproducer *Ashbya gossypii*, Biotechnol. Bioeng., **111,** 1191–1199 (2014).
31. **Monschau, N., Sahm, H., and Stahmann, K.:** Threonine aldolase overexpression plus threonine supplementation enhanced riboflavin production in *Ashbya gossypii*, Appl. Environ. Microbiol., **64,** 4283–4290 (1998).
32. **Schlösser, T., Wiesenburg, A., Gätgens, C., Funke, A., Viets, U., Vijayalakshmi, S.,**

**Nieland, S., and Stahmann, K.P.:** Growth stress triggers riboflavin overproduction in *Ashbya gossypii*, Appl. Microbiol. Biotechnol., **76,** 569–578 (2007).

33. **Sugimoto, T., Kanamasa, S., Kato, T., and Park, E.Y.:** Importance of malate synthase in the glyoxylate cycle of *Ashbya gossypii* for the efficient production of riboflavin, Appl. Microbiol. Biotechnol., **83,** 529–539 (2009).

34. **Schlüpen, C., Santos, M.A., Weber, U., de Graaf, A., Revuelta, J.L., and Stahmann, K.P.:** Disruption of the SHM2 gene, encoding one of two serine hydroxymethyltransferase isozymes, reduces the flux glycine to serine in *Ashbya gossypii*, Biochem. J., **369,** 263-273 (2003).

# FIGURE LEGENDS

FIG. 1. Time course of *A. gossypii* cultivation in 500-mL Erlenmeyer flasks. *A. gossypii* wild type (A) and mutant (B) strains were cultured on minimal medium containing GLC and ASN as carbon and nitrogen sources, respectively. Closed circles, DCW; open circles, RIB concentration; closed triangle, LAC concentration; closed squares, GLC concentration; open squares, ASN concentration.

FIG 2. *In vivo* carbon flux distribution in the central metabolic pathway of wild type (top) and high RIB-producing *A. gossypii* (bottom) strains. *A. gossypii* wild type and mutant strains were cultured on GLC and ASN. The fluxes were determined from the best fit of GC-MS labeling of amino acids from cellular proteins in cultures cultivated with [1, 2-$^{13}$C]-labeled GLC and unlabeled ASN using a comprehensive approach of combined metabolite balancing and isotopomer. For reversible reactions, the direction of the net flux in square boxes is indicated by an additional arrow beside the corresponding reaction. Numbers indicate flux reversibility. All fluxes are presented as a molar percentage of the specific GLC uptake rate. The data are presented as flux ± random error. Abbreviations: 3PG, glycerate 3-phophate; AcCoA, acetyl-CoA; ACE, acetate; ACETAL, acetaldehyde; AKG, α-ketoglutarate; ALA, alanine; ANAPL, anaplerotic pathway; ASN, asparagine; ASP, aspartate; DHAP, dihydroxyacetone phosphate; E4P, erythrose 4-phosphate; EMP, Embden–Meyerhof–Parnas pathway; F6P, fructose 6-phosphate; GAP, glyceraldehyde 3-phosphate; G6P, glucose 6-phosphate; GLC, glucose; GLU, glutamate; GLY, glycine; GTP, guanosine triphosphate; LAC, lactate; MAL, malate; MFA, Metabolic flux analysis, MTHF, methylenetetrahydrofolate; OAA, oxaloacetate; P5P, pentose 5-phosphate; PEP, phosphoenolpyruvate; PPP, pentose phosphate pathway; PSP, purine synthesis pathway; PYR, pyruvate; RIB, riboflavin; S7P, sedoheptulose 7-phosphate; SER, serine; SUC, succinate; TCA, tricarboxylic acid cycle;

417 THR, threonine; $V_1$-$V_{58}$, stoichiometric reactions. Subscripts; cyt; cytosol; ex, extracellular;

418 mit, mitochondria.

**TABLE 1.** Specific growth rate and yield parameters for wild type and mutant *A.* strains.

| Parameter | Wild type | Mutant |
|---|---|---|
| $\mu$ [$d^{-1}$] | 1.014 ± 0.003 | 0.783 ± 0.001 |
| Specific consumption rate of GLC* [mmol/g DCW/d] | 21.574 ± 0.002 | 12.429 ± 0.003 |
| Specific consumption rate of ASN* [mmol/g DCW/d] | 15.134 ± 0.005 | 2.333 ± 0.004 |
| Specific production rate of RIB* [mmol/g DCW/d] | 0.018 ± 0.002 | 0.116 ± 0.002 |
| Specific production rate of LAC* [mmol/g DCW/d] | 0.809 ± 0.002 | 1.656 ± 0.001 |
| *Yield coefficients* | | |
| $Y_{x/GLC}$ [g/mmol] | 0.047 ± 0.001 | 0.063 ± 0.004 |
| $Y_{RIB/GLC}$ [mmol/mmol] | 0.001 ± 0.000 | 0.016 ± 0.002 |
| $Y_{LAC/GLC}$ [mmol/mmol] | 0.038 ± 0.001 | 0.168 ± 0.001 |
| $Y_{ACE/GLC}$ [mmol/mmol] | 0.028 ± 0.003 | 0.037 ± 0.001 |
| $Y_{AKG/GLC}$ [mmol/mmol] | 0.053 ± 0.002 | 0.047 ± 0.006 |
| $Y_{ALA/GLC}$ [mmol/mmol] | 0.006 ± 0.001 | 0.018 ± 0.001 |
| $Y_{GLU/GLC}$ [mmol/mmol] | 0.014 ± 0.003 | 0.014 ± 0.006 |
| $Y_{PYP/GLC}$ [mmol/mmol] | 0.023 ± 0.003 | 0.066 ± 0.002 |
| $Y_{SUC/GLC}$ [mmol/mmol] | 0.009 ± 0.006 | 0.005 ± 0.003 |

* Obtained in exponential growth phase.

Data are presented as the mean of the specific rate ± standard error from three parallel cultivation experiments.

**TABLE 2.** Relative mass isotopomer fractions of amino acids from the cellular proteins of *A. gossypii* wild type strain cultivated on 99% [1, 2-$^{13}$C] glucose and unlabeled asparagine.

| Amino acid | | Mass isotopomers | | | |
|---|---|---|---|---|---|
| | | $M_0$ | $M_1$ | $M_2$ | $M_3$ |
| Alanine | Calc | 0.418 | 0.144 | 0.352 | 0.086 |
| (*m/z* 260) | Exp | 0.444 ±0.002 | 0.158 ± 0.003 | 0.301 ± 0.003 | 0.097 ± 0.004 |
| Valine | Calc | 0.249 | 0.202 | 0.297 | 0.140 |
| (*m/z* 288) | Exp | 0.294 ± 0.010 | 0.147 ± 0.009 | 0.302 ± 0.015 | 0.120 ± 0.017 |
| Aspartate | Calc | 0.429 | 0.219 | 0.207 | 0.106 |
| (*m/z* 418) | Exp | 0.392 ± 0.003 | 0.243 ± 0.002 | 0.196 ± 0.003 | 0.116 ± 0.005 |
| Glutamate | Calc | 0.253 | 0.227 | 0.270 | 0.143 |
| (*m/z* 432) | Exp | 0.187 ± 0.003 | 0.203 ± 0.000 | 0.261 ± 0.003 | 0.185 ± 0.004 |
| Serine | Calc | 0.364 | 0.290 | 0.254 | 0.091 |
| (*m/z* 390) | Exp | 0.376 ± 0.004 | 0.267 ± 0.003 | 0.253 ± 0.003 | 0.104 ± 0.000 |
| Phenylalanine | Calc | 0.157 | 0.122 | 0.272 | 0.168 |
| (*m/z* 336) | Exp | 0.191 ± 0.002 | 0.137 ± 0.001 | 0.243 ± 0.002 | 0.152 ± 0.001 |
| Glycine | Calc | 0.586 | 0.312 | 0.102 | |
| (*m/z* 246) | Exp | 0.559 ± 0.002 | 0.302 ± 0.001 | 0.139 ± 0.012 | |
| Tyrosine | Calc | 0.136 | 0.121 | 0.253 | 0.177 |
| (*m/z* 466) | Exp | 0.166 ± 0.006 | 0.137 ± 0.008 | 0.229 ± 0.010 | 0.156 ± 0.002 |
| Threonine | Calc | 0.429 | 0.220 | 0.206 | 0.106 |
| (*m/z* 466) | Exp | 0.395 ± 0.001 | 0.243 ± 0.002 | 0.197 ± 0.003 | 0.113 ± 0.005 |
| Lysine (*m/z* | Calc | 0.168 | 0.235 | 0.255 | 0.184 |
| 431) | Exp | 0.191 ± 0.002 | 0.181 ± 0.006 | 0.242 ± 0.001 | 0.176 ± 0.006 |
| Arginine | Calc | 0.187 | 0.233 | 0.257 | 0.175 |
| (*m/z* 442) | Exp | 0.207 ± 0.005 | 0.205 ± 0.005 | 0.236 ± 0.002 | 0.170 ± 0.006 |

The data shown represent experimental GC-MS results with standard deviation (Exp) and values predicted by the solution of the mathematical model corresponding to the optimized set of fluxes (Calc). Amino acids were analyzed by GC-MS as MBDSTFA derivatives.

**TABLE 3.** Relative mass isotopomer fractions of amino acids from the cellular proteins of *A. gossypii* mutant strain cultivated on 99% [1, 2-$^{13}$C] glucose and unlabeled asparagine.

| Amino acid | | Mass isotopomers | | | |
|---|---|---|---|---|---|
| | | $M_0$ | $M_1$ | $M_2$ | $M_3$ |
| Alanine | Calc | 0.423 | 0.152 | 0.343 | 0.082 |
| (*m/z* 260) | Exp | 0.473 ± 0.001 | 0.154 ± 0.003 | 0.289 ± 0.000 | 0.084 ± 0.000 |
| Valine | Calc | 0.243 | 0.196 | 0.301 | 0.143 |
| (*m/z* 288) | Exp | 0.333 ± 0.002 | 0.146 ± 0.001 | 0.296 ± 0.002 | 0.106 ± 0.003 |
| Aspartate | Calc | 0.604 | 0.226 | 0.122 | 0.037 |
| (*m/z* 418) | Exp | 0.607 ± 0.001 | 0.224 ± 0.002 | 0.118 ± 0.001 | 0.038 ± 0.003 |
| Glutamate | Calc | 0.242 | 0.238 | 0.269 | 0.147 |
| (*m/z* 432) | Exp | 0.218 ± 0.001 | 0.208 ± 0.003 | 0.263 ± 0.001 | 0.170 ± 0.003 |
| Serine | Calc | 0.401 | 0.248 | 0.261 | 0.090 |
| (*m/z* 390) | Exp | 0.415 ± 0.005 | 0.235 ± 0.004 | 0.254 ± 0.004 | 0.097 ± 0.000 |
| Phenylalanine | Calc | 0.175 | 0.136 | 0.281 | 0.165 |
| (*m/z* 336) | Exp | 0.234 ± 0.002 | 0.142 ± 0.000 | 0.245 ± 0.000 | 0.145 ± 0.002 |
| Glycine | Calc | 0.597 | 0.304 | 0.098 | |
| (*m/z* 246) | Exp | 0.588 ± 0.000 | 0.266 ± 0.000 | 0.146 ± 0.000 | |
| Tyrosine | Calc | 0.151 | 0.135 | 0.262 | 0.175 |
| (*m/z* 466) | Exp | 0.200 ± 0.010 | 0.142 ± 0.007 | 0.235 ± 0.008 | 0.152 ± 0.003 |
| Threonine | Calc | 0.462 | 0.224 | 0.191 | 0.091 |
| (*m/z* 466) | Exp | 0.432 ± 0.002 | 0.241 ± 0.000 | 0.187 ± 0.004 | 0.098 ± 0.001 |
| Lysine | Calc | 0.155 | 0.239 | 0.257 | 0.189 |
| (*m/z* 431) | Exp | 0.193 ± 0.001 | 0.176 ± 0.004 | 0.235 ± 0.001 | 0.179 ± 0.004 |
| Arginine | Calc | 0.181 | 0.238 | 0.260 | 0176 |
| (*m/z* 442) | Exp | 0.195 ± 0.014 | 0.236 ± 0.016 | 0.185 ± 0.001 | 0.156 ± 0.006 |

The data shown represent experimental GC-MS results with standard deviation (Exp) and values predicted by the solution of the mathematical model corresponding to the optimized set of fluxes (Calc). Amino acids were analyzed by GC-MS as MBDSTFA derivatives.

**Supplementary materials**

**Table S1.** Precursor stoichiometry for biomass formation

| | Wild type ($\mu$=1.014 $d^{-1}$) (mmol/g DCW) | Mutant ($\mu$=0.783 $d^{-1}$) (mmol/g DCW) |
|---|---|---|
| G6P | 4.009 ± 0.612 | 3.731 ± 0.600 |
| GLY | 1.186 ± 0.100 | 1.104 ± 0.100 |
| P5P | 1.114 ± 0.301 | 1.037 ± 0.303 |
| E4P | 0.809 ± 0.400 | 0.753 ± 0.401 |
| G3P | 0.219 ± 0.100 | 0.203 ± 0.100 |
| SER | 0.588 ± 0.504 | 0.547 ± 0.100 |
| PEP | 1.618 ±0.503 | 1.506 ± 0.509 |
| $PYR_{cyt}$ | 5.330 ± 0.600 | 4.960 ± 0.600 |
| $AcCoA_{cyt}$ | 6.002 ± 0.200 | 5.585 ± 0.200 |
| $AcCoA_{mit}$ | 0.908 ± 0.110 | 0.844 ± 0.100 |
| $OAA_{cyt}$ | 1.717 ± 0.100 | 1.597 ± 0.100 |
| AKG | 3.121 ± 0.200 | 2.904 ± 0.200 |
| THR | 1.176 ± 0.301 | 1.095 ± 0.305 |

Data were calculated based on reference (1) and are shown average ± standard deviation.

**TABLE S2.** Stoichiometry of metabolic reactions in riboflavin-producing *Ashbya gossypii*.

| Metabolite | Overall reaction |
|---|---|
| Glucose 6-phosphate (G6P) | $V_1-V_9-V_{14}-V_{46}=0$ |
| Fructose 6-phosphate (F6P) | $V_8-V_9+V_{17}-V_{18}+V_{19}=0$ |
| Pentose 5-phosphate (P5P) | $V_{14}-V_{19}-V_{47}-2V_{15}+2V_{16}-V_{20}=0$ |
| Erythrose 4-phosphate (E4P) | $V_{17}-V_{18}-V_{19}-V_{48}=0$ |
| Sedoheptulose 7-phosphate (S7P) | $V_{15}-V_{16}-V_{17}+V_{18}=0$ |
| Glyceraldehyde 3-phophate (GAP) | $V_9+V_{10}-V_{11}+V_{15}-V_{16}-V_{17}+V_{18}-V_{49}=0$ |
| Glycerate 3-phosphate (G3P) | $V_{11}-V_{12}-V_{20}-V_{21}=0$ |
| Phophoenol-pyruvate (PEP) | $V_{12}-V_{13}-V_{50}=0$ |
| Pyruvate cyt ($PYR_{cyt}$) | $V_{13}-V_{31}-V_{34}-V_{40}-V_{41}-V_{45}=0$ |
| Pyruvate mit ($PYR_{mit}$) | $V_{33}-V_{25}+V_{30}=0$ |
| Acetyl-CoA mit ($AcCoA_{mit}$) | $V_{25}-V_{26}-V_{57}=0$ |
| Acetyl-CoA cyt ($AcCoA_{cyt}$) | $V_7+V_{36}-V_{56}=0$ |
| α-ketoglutarate (AKG) | $V_{26}-V_{27}-V_{42}-V_{43}-V_{51}=0$ |
| Succinate (SUC) | $V_{27}-V_{28}-V_{44}=0$ |
| Malate (MAL) | $V_{28}-V_{29}-V_{30}=0$ |
| Oxaloacetate mit ($OAA_{mit}$) | $V_{29}-V_{26}+V_{32}=0$ |
| Oxaloacetate cyt ($OAA_{cyt}$) | $V_3-V_4-V_6+V_{31}-V_{32}-V_{55}=0$ |
| Guanosine triphosphate (GTP) | $V_{20}-V_{24}=0$ |
| Serine (SER) | $V_{21}-V_{22}-V_{53}=0$ |
| Threonine (THR) | $V_5+V_6-V_7-V_{54}=0$ |
| Acetaldehyde (ACETAL) | $V_{34}-V_{35}=0$ |
| Acetate (ACE) | $V_{35}-V_{36}-V_{37}=0$ |
| Aspartate (ASP) | $V_2-V_3+V_4-V_5=0$ |
| Glycine (GLY) | $V_7+V_{22}-V_{23}-V_{52}=0$ |

**Table S3.** Metabolic network for *A. gossypii*. The model file is present with constraints to simulate riboflavin production from glucose.

*Glucose uptake*

| | | | |
|---|---|---|---|
| *v*1 | GlC_EX (abcdef) | → | G6P (abcdef) |

*Asparagin, threonine and glycine metabolism*

| | | | |
|---|---|---|---|
| *v*2 | ASN_EX (abcd) | → | ASP (abcd) |
| *v*3/ *v*4 | ASP (abcd) | ↔ | $OAA_{cyt}$ (abcd) |
| *v*5 | ASP (abcd) | → | THR (abcd) |
| *v*6 | $OAA_{cyt}$ (abcd) | → | THR (abcd) |
| *v*7 | THR (abcd) | → | GLY (ab) + $AcCoA_{cyt}$ (cd) |

*Glycolysis*

| | | | |
|---|---|---|---|
| *v*8 | G6P (abcdef) | → | F6P (abcdef) |
| *v*9 | F6P (abcdef) + ATP (X) | → | DHAP (abc) + G3P (def) |
| *v*10 | DHAP (abc) | → | G3P (cba) |
| *v*11 | G3P (abc) | → | 3PG (abc) + ATP (X) + NADH (X) |
| *v*12 | 3PG (abc) | → | PEP (abc) |
| *v*13 | PEP (abc) | → | $PYR_{cyt}$ (abc) + ATP (X) |

*Pentose phosphate pathway*

| | | | |
|---|---|---|---|
| *v*14 | G6P (abcdef) | → | P5P (abcde) + $CO_2$ (f) + 2NADPH (2X) |
| *v*15/*v*16 | P5P (abcde) + P5P (fghij) | ↔ | S7P (fgabcde) + G3P (hij) |
| *v*17/*v*18 | S7P (abcdefg) + G3P (hij) | ↔ | E4P (defg) + F6P (abchij) |
| *v*19 | E4P (abcd) + P5P (efghi) | → | F6P (efabcd) + G3P (ghi) |
| *v*20 | P5P (abcde) + 3PG (fgh) + 2MTHF (ij) | → | GTP (abcdefghij) |
| *v*21 | 3PG (abc) | → | SER (abc) |
| *v*22 | SER (abc) | → | GLY (ab) + MTHF (c) |
| *v*23 | GLY (ab) | → | MTHF (a) + $CO_2$ (b) |

*Riboflavin Formation*

| | | | |
|---|---|---|---|
| *v*24 | GLY | → | RIB_EX ($B^{*1}$) |

*TCA cycle*

| | | | |
|---|---|---|---|
| *v*25 | $PYR_{mit}$ (abc) | → | $ACCOA_{mit}$ (bc) + $CO_2$ (a) + NADH (X) |
| *v*26 | $AcCoA_{mit}$ (ab) + $OAA_{mit}$ (cdef) | → | AKG (abcde) + $CO_2$ (f) + NADPH (X) |
| *v*27 | AKG (abcde) | → | 0.5SUC (bcde) + 0.5SUC (edcd) + $CO_2$ (a) + NADH (X) + ATP (X) |
| *v*28 | SUC (abcd) | → | MAL (abcd) + NADH (X) |
| *v*29 | MAL (abcd) | → | $OAA_{mit}$ (abc) + NADH (X) |
| *v*30 | MAL (abcd) | → | $PYR_{mit}$ (abc) + $CO_2$ (d) + NADPH (X) |

*Transport reactions cytosol-mitochondria*

| | | | |
|---|---|---|---|
| *v*31 | $PYR_{cyt}$ (abc) + $CO_2$ (d) + ATP (X) | → | $OAA_{cyt}$ (abcd) |
| *v*32 | $OAA_{cyt}$ (abc) | → | $OAA_{mit}$ (abc) |
| *v*33 | $PYR_{cyt}$ (abc) | → | $PYR_{mit}$ (abc) |
| *v*34 | $PYR_{cyt}$ (abc) | → | ACETAL (bc) + $CO_2$ (a) |

*Formation of AcCoA in the cytosol*

| | | | |
|---|---|---|---|
| *v*35 | ACETAL (ab) | → | ACE (ab) |
| *v*36 | ACE (ab) | → | $AcCoA_{cyt}$ (ab) |
| *v*37 | ACE | → | ACE_EX ($B^{*1}$) |

*$CO_2$ formation*

| | | | |
|---|---|---|---|
| v38/v39 | $CO_2$ (a) | ↔ | $CO_2$_EX (a) |

*Biomass formation*

| | | | |
|---|---|---|---|
| *v*40 | $PYR_{cyt}$ | → | $PYR_{cyt}$_EX ($B^{*1}$) |
| *v*41 | $PYR_{cyt}$ | → | LAC_EX ($B^{*1}$) |
| *v*42 | AKG | → | AKG_EX ($B^{*1}$) |
| *v*43 | AKG | → | GLU_EX ($B^{*1}$) |
| *v*44 | SUC | → | SUC_EX ($B^{*1}$) |
| *v*45 | $PYR_{cyt}$ | → | ALA_EX ($B^{*1}$) |
| *v*46 | G6P | → | G6P_B ($B^{*1}$) |
| *v*47 | P5P | → | P5P_B ($B^{*1}$) |
| *v*48 | E4P | → | E4P_B ($B^{*1}$) |
| *v*49 | G3P | → | G3P_B ($B^{*1}$) |
| *v*50 | PEP | → | PEP_B ($B^{*1}$) |
| *v*51 | AKG | → | AKG_B ($B^{*1}$) |
| *v*52 | GLY | → | GLY_B ($B^{*1}$) |

| | | | |
|---|---|---|---|
| *v*53 | SER | → | SER_B (B*[1]) |
| *v*54 | THR | → | THR_B (B*[1]) |
| *v*55 | $OAA_{cyt}$ | → | $OAA_{cyt}$_B (B*[1]) |
| *v*56 | $AcCoA_{cyt}$ | → | $AcCoA_{cyt}$_B (B*[1]) |
| *v*57 | $AcCoA_{mit}$ | → | $AcCoA_{mit}$_B (B*[1]) |
| *v*58 | $PYR_{cyt}$ | → | $PYR_{cyt}$_B (B*[1]) |

*Amino acid synthesis*

| | | | |
|---|---|---|---|
| *v*59 | GLY (ab) + MTHF (c) | → | SER (abc) (S*[2]) |
| *v*60 | PYRmit (abc) + PYRmit (def) | → | VAL (abcde) + $CO_2$ (f) (S*[2]) |
| *v*61 | E4P (abcd) + PEP (efg) | → | SHKM (efgabcd) (S*[2]) |
| *v*62 | SHKM (abcdefg) + PEP (hij) | → | CHRM (abcdefghij) (S*[2]) |
| *v*63 | CHRM (abcdefghij) | → | PHE (hijbcdefg) + $CO_2$ (a) (S*[2]) |
| *v*64 | CHRM (abcdefghij) | → | TYR (hijbcdefg) + $CO_2$ (a) (S*[2]) |
| *v*65 | CHRM (abcdefghij) | → | ANTHR (abcdefg) + PYR (hij) (S*[2]) |
| *v*66 | ANTHR (abcdefg) +P5P (hijkl) | → | CPADR5P (abcdefghijkl) (S*[2]) |
| *v*67 | CPADR5P (abcdefghijkl) | → | INDG (abcdfghijkl) + $CO_2$ (e) (S*[2]) |
| *v*68 | INDG (abcdefghijk) | → | IND (abcdefgh) + G3P (ijk) (S*[2]) |
| *v*69 | IND (abcdefgh) + SER (ijk) | → | TRP (abcdefghkji) (S*[2]) |
| *v*70 | $PYR_{mit}$ (abc) + $PYR_{mit}$ (def) | → | ISV (abefc) + $CO_2$ (d) (S*[2]) |
| *v*71 | ISV (abcde) +$AcCoA_{mit}$ (fg) | → | LYS (abcdeg) + $CO_2$ (f) (S*[2]) |
| *v*72 | AKG (abcde) + $CO_2$ (f) | → | ARG (abcdef) (S*[2]) |
| *v*73 | AKG (abcde) + $AcCoA_{mit}$ (fg) | → | LYS (abcdeg) + $CO_2$ (f) (S*[2]) |
| *v*74 | $OAA_{cyt}$ (abcd) + MTHF (e) | → | MET (abcde) (S*[2]) |
| *v*75 | P5P (abcde) + MTHF (f) | → | HIS (edcbaf) (S*[2]) |
| *v*76 | 3PG (abc) | → | CYS ( abc) (S*[2]) |
| *v*77 | PYR (abc) | → | ALA (abc) (S*[2]) |
| *v*78 | $OAA_{cyt}$ (abcd) | → | APN (abcd) (S*[2]) |
| *v*79 | $OAA_{cyt}$ (abcd) | → | ASP (abcd) (S*[2]) |
| *v*80 | $PYR_{mit}$ (abc) + $OAA_{mit}$ (defg) | → | ILE (debfgc) + $CO_2$ (a) (S*[2]) |
| *v*81 | AKG (abcde) | → | GLU (abcde) (S*[2]) |
| *v*82 | AKG (abcde) | → | GLN (abcde) (S*[2]) |
| *v*83 | AKG (abcde) | → | PRO (abcde) (S*[2]) |

*[1] “B” means the reaction that is to be excluded from isotopomer balance, typically

reactions that drain biomass precursors.
*[2] “S” means the reaction that is to be excluded from metabolite balance. This type of reaction is used to map label distribution of the measured metabolites to their precursors.

| *Precursor* | |
|---|---|
| 3PG | glycerate 3-phophate |
| ACE | acetate |
| AcCoA | acetyl-CoA |
| ACETAL | acetaldehyde |
| AKG | α-ketoglutarate |
| ALA | alanine |
| ASN | asparagine |
| ARG | arginine |
| ASP | aspartate |
| ANTHR | anthranilate |
| CHRM | chorismate |
| CPADR5P | 1-(o-carboxyphenylamino)-1-deoxyribuose 5-phosphate |
| CYS | cysteine |
| DHAP | dihydroxyacetone phosphate |
| E4P | erythrose 4-phosphate |
| F6P | fructose 6-phosphate |
| GAP | glyceraldehyde 3-phosphate |
| G6P | glucose 6-phosphate |
| GLC | glucose |
| GLU | glutamate |
| GLN | glutamine |
| GLY | glycine |
| GTP | guanosine triphosphate |
| HIS | histidine |
| ILE | isoleucine |

| | |
|---|---|
| IND | indole |
| INDG | indole-3-glyserinphophate |
| ISV | isovaline |
| LAC | lactate |
| LYS | lysine |
| MAL | malate |
| MET | methionine |
| MTHF | methylenetetrahydrofolate |
| OAA | oxaloacetate |
| P5P | pentose 5-phosphate |
| PEP | phosphoenolpyruvate |
| PHE | phenylalanine |
| PRO | proline |
| PYR | pyruvate |
| RIB | riboflavin |
| S7P | sedoheptulose 7-phophate |
| SER | serine |
| SHKM | shikimate |
| SUC | succinate |
| THR | threonine |
| TRP | tryptophan |

## Reference

1. **Gombert, A.K., Santos, M.A., Christensen, B., Nielsen, J.:** Network identification and flux quantification in the central metabolism of Saccharomyces cerevisiae under different conditions of glucose repression, J. Bacteriol., **183**: 1441–1451 (2001).

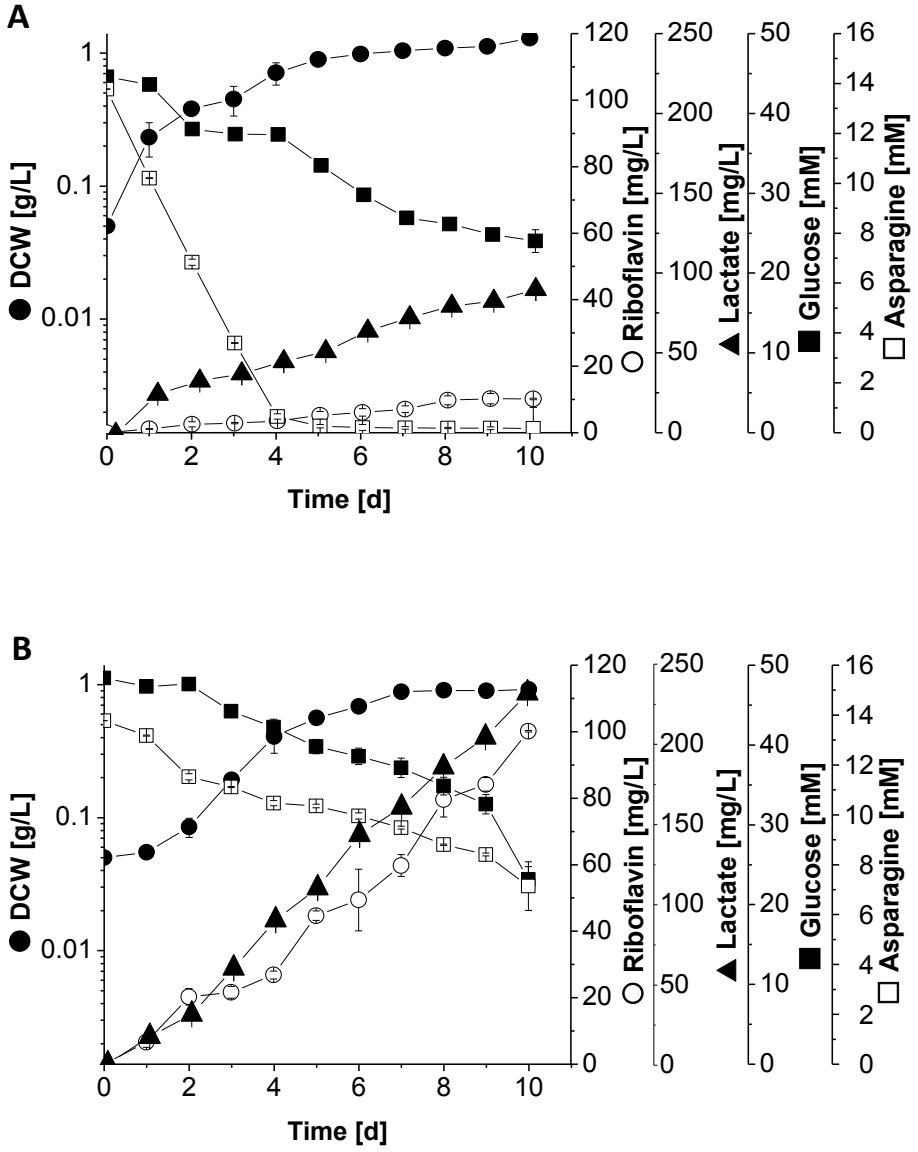
A
B
DCW [g/L]
Riboflavin [mg/L]
Lactate [mg/L]
Glucose [mM]
Asparagine [mM]
Time [d]
0
2
4
6
8
10
0.01
0.1
1
20
40
60
80
100
120
50
150
200
250
12
14
16

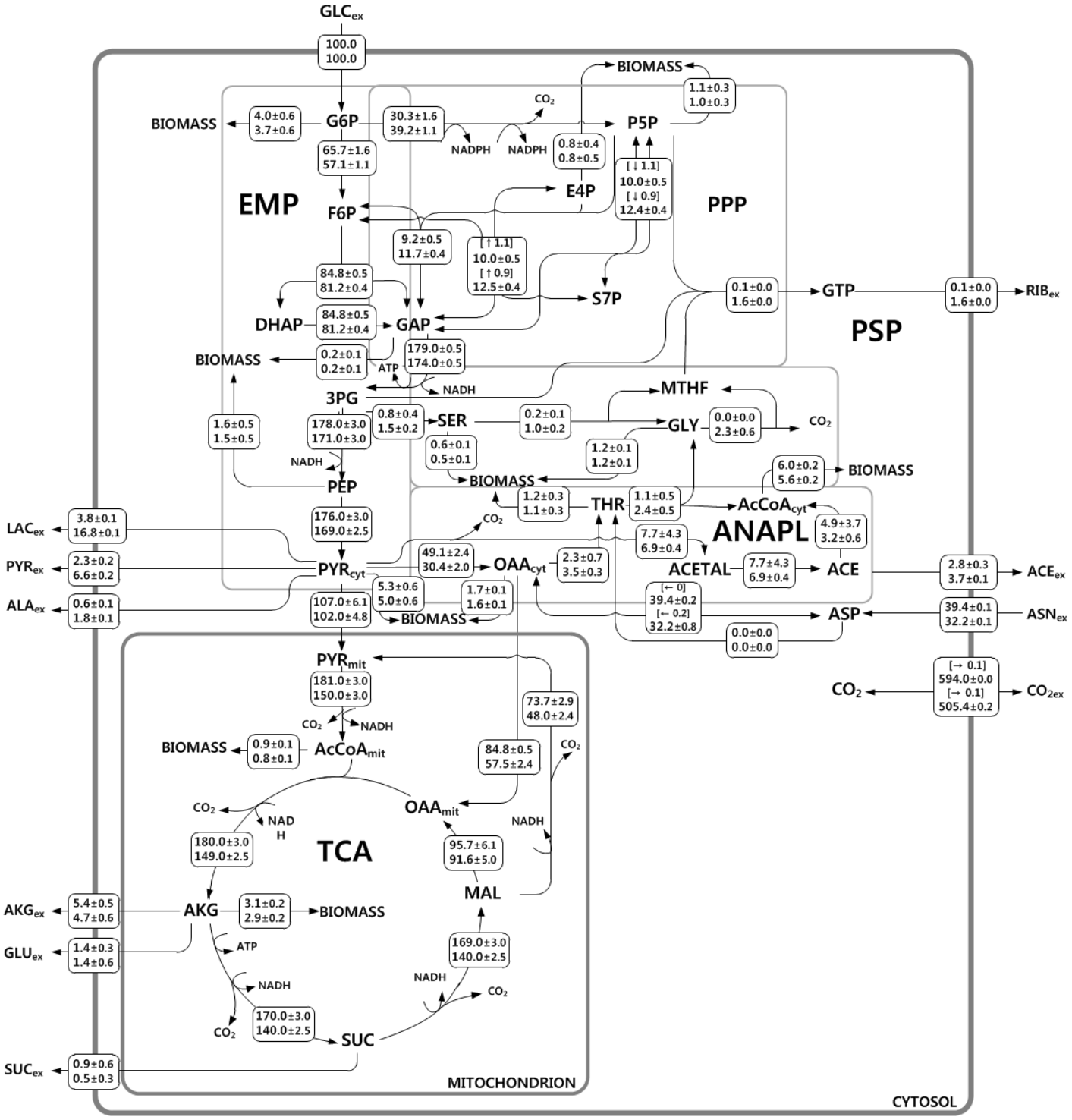
GLC_ex
100.0
100.0
BIOMASS
1.1±0.3
1.0±0.3
BIOMASS
4.0±0.6
3.7±0.6
G6P
30.3±1.6
39.2±1.1
CO2
NADPH
NADPH
P5P
0.8±0.4
0.8±0.5
65.7±1.6
57.1±1.1
E4P
[↓1.1]
10.0±0.5
[↓0.9]
12.4±0.4
EMP
F6P
PPP
9.2±0.5
11.7±0.4
[↑1.1]
10.0±0.5
[↑0.9]
12.5±0.4
84.8±0.5
81.2±0.4
S7P
0.1±0.0
1.6±0.0
GTP
0.1±0.0
1.6±0.0
RIB_ex
DHAP
84.8±0.5
81.2±0.4
GAP
PSP
BIOMASS
0.2±0.1
0.2±0.1
ATP
179.0±0.5
174.0±0.5
NADH
MTHF
3PG
1.6±0.5
1.5±0.5
178.0±3.0
171.0±3.0
0.8±0.4
1.5±0.2
SER
0.2±0.1
1.0±0.2
GLY
0.0±0.0
2.3±0.6
CO2
0.6±0.1
0.5±0.1
1.2±0.1
1.2±0.1
NADH
BIOMASS
6.0±0.2
5.6±0.2
BIOMASS
PEP
1.2±0.3
1.1±0.3
THR
1.1±0.5
2.4±0.5
AcCoA_cyt
LAC_ex
3.8±0.1
16.8±0.1
176.0±3.0
169.0±2.5
CO2
ANAPL
4.9±3.7
3.2±0.6
7.7±4.3
6.9±0.4
PYR_ex
2.3±0.2
6.6±0.2
PYR_cyt
49.1±2.4
30.4±2.0
OAA_cyt
2.3±0.7
3.5±0.3
ACETAL
7.7±4.3
6.9±0.4
ACE
2.8±0.3
3.7±0.1
ACE_ex
ALA_ex
0.6±0.1
1.8±0.1
5.3±0.6
5.0±0.6
1.7±0.1
1.6±0.1
[← 0]
39.4±0.2
[← 0.2]
32.2±0.8
ASP
39.4±0.1
32.2±0.1
ASN_ex
107.0±6.1
102.0±4.8
BIOMASS
0.0±0.0
0.0±0.0
PYR_mit
[→ 0.1]
594.0±0.0
[→ 0.1]
505.4±0.2
CO2
CO2ex
181.0±3.0
150.0±3.0
73.7±2.9
48.0±2.4
CO2
NADH
BIOMASS
0.9±0.1
0.8±0.1
AcCoA_mit
84.8±0.5
57.5±2.4
CO2
CO2
OAA_mit
NAD
H
NADH
180.0±3.0
149.0±2.5
TCA
95.7±6.1
91.6±5.0
MAL
AKG_ex
5.4±0.5
4.7±0.6
AKG
3.1±0.2
2.9±0.2
BIOMASS
GLU_ex
1.4±0.3
1.4±0.6
ATP
169.0±3.0
140.0±2.5
NADH
NADH
CO2
CO2
170.0±3.0
140.0±2.5
SUC
SUC_ex
0.9±0.6
0.5±0.3
MITOCHONDRION
CYTOSOL